

Joint Inversion – A Solution to the Imaging Challenges of Fold & Thrust Belt (FTB)

Ashok Kumar Pandey¹, Dr. Uma Shankar¹, Pawan Kumar Singh², Dr. Rajeev Bhatla¹, 1. Department of Geophysics BHU India, 2. Oil India Limited, Duliajan, India

Abstract

Seismic exploration has revolutionized the field of hydrocarbon exploration since its advent. Furthermore, as the “easy” or conventional hydrocarbon resources have been studied to their exhaustion, the exploration has moved towards unconventional and geologically challenging settings like Fold thrust belts and sub-salt, sub-basalt geology, etc. This high-resolution seismic acquisition and imaging suffer from illumination and noise problems along with incorrect parameter estimation in these settings. However, the potential field data has no such limitation in this complex geological area so, their complementary properties are used in the form of Joint inversion to image the sub-surface geology.

Joint Inversion of geophysical data has become increasingly popular for many different applications as it can efficiently combine complementary information from different datasets (Moorkamp,2010). Consequently, with joint inversion of multiple geophysical data, the model parameter estimation is constrained to be less ambiguous and close to the true geological conditions. Thus, one can carry out a more reliable and integrated interpretation of the data and model parameter distribution.

The major component and a promising field of research in the domain of Joint Inversion is the coupling function that connects two or more entirely different geophysical data. Broadly, the coupling mechanism can be categorized into rock physics (petrophysical) and structural. Rock-physics coupling operators are based on empirical relations between two different geophysical parameters and could be derived from cross-plot analysis (Gardner,1974). The structure coupling works in a different manner by imposing a similarity between the spatial distribution of the model parameters in the sub-surface. One of the most popular structural coupling mechanisms is cross-gradient (Gallardo & Meju,2003,2004). The cross-gradient operator basically compels different model parameters to be similar in structures by forcing the parallelism of gradient directions.

In our work titled “Integrated Seismic Imaging and Joint Inversion,” we studied and applied cross-gradient-based geophysical joint inversion as an integral step in the depth-imaging workflow of the seismic data for a fault & thrust belt (FTB) region with poor seismic SNR. Seismic refraction data were inverted jointly with Bouguer Anomaly data to derive accurate interval velocity and density volumes for the region. The models were assessed with velocity and density logs. Further, a Pre-Stack Kirchhoff Depth Migration was performed using the velocity model and it was compared with Depth migrated gathers that were migrated using Interval velocity from seismic grid tomography.

Keywords: Joint Inversion, Fold Thrust Belt, Potential Field data

JOINT INVERSION

Joint Inversion of geophysical data has become increasingly popular for many different applications (e.g., Oil Exploration, Hydrology and Mining) since it efficiently combines complementary information from different geophysical data sets (Moorkamp,2010). Consequently, with joint inversion of multiple geophysical data, the model parameter estimated is constrained to be less ambiguous and close to the true geological conditions. Joint Inversion has moved ahead from a nascent idea to developing stage, where many technical aspects have been developed to handle multiple combinations of data, model parameters, and constraints.

This project under study aims at integrating seismic data (first arrival travel time) with potential field data (gravity and magnetics) to improve the velocity field that improves the pre-stack depth migrated gathers and stacks. This approach can be a game-changer, especially for seismic data acquired in difficult settings like Fold Thrust Belt and for sub-basalt prospects, where seismic data is contaminated with noise and the sub-surface cannot be imaged reliably with the best resolution.

Theoretical Foundation for Joint Inversion

There are two popular strategies to combine different geophysical data and using the individual data to complement the other during inversion.

The first strategy is to sequentially perform an inversion on each data independently while enhancing their similarity by sharing information between different inversion iterations. This is called *Cooperative Joint Inversion (CJI)*. The second strategy is called *simultaneous joint inversion (SJI)* which takes more than one type of data as inputs simultaneously and minimizes a composite objective function in a single inversion run.

While our goal is to perform Simultaneous Joint Inversion (SJI), it is unaffordable to run SJI right from the beginning as there are many parameters involved and it is almost impossible to test them simultaneously, so instead of performing SJI at the very beginning, we started with first break travel-time inversion and gravity inversion, sequentially and cooperatively. Sequential (CJI) inversions can be run at the beginning when there is still room to improve the initial models by individual inversion of

first arrival time (refraction) and gravity anomaly data.

CJI could be considered a valuable parameter testing stage for SJI. It is practical and better to test geophysical parameters during CJI and the weightings (trade-off parameters and constraint) during SJI. CJI provides benchmark models which are important to assess the output of SJI. SJI is necessary because the only coupling mechanism in CJI is Gardner's relation to sharing information between velocity and density models. SJI provides more explicit constraints to exchange information between models.

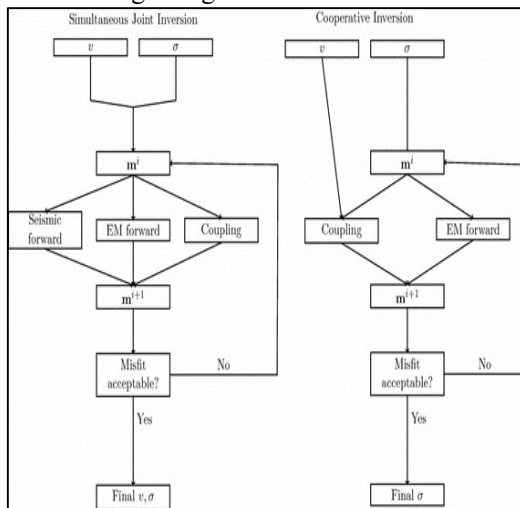


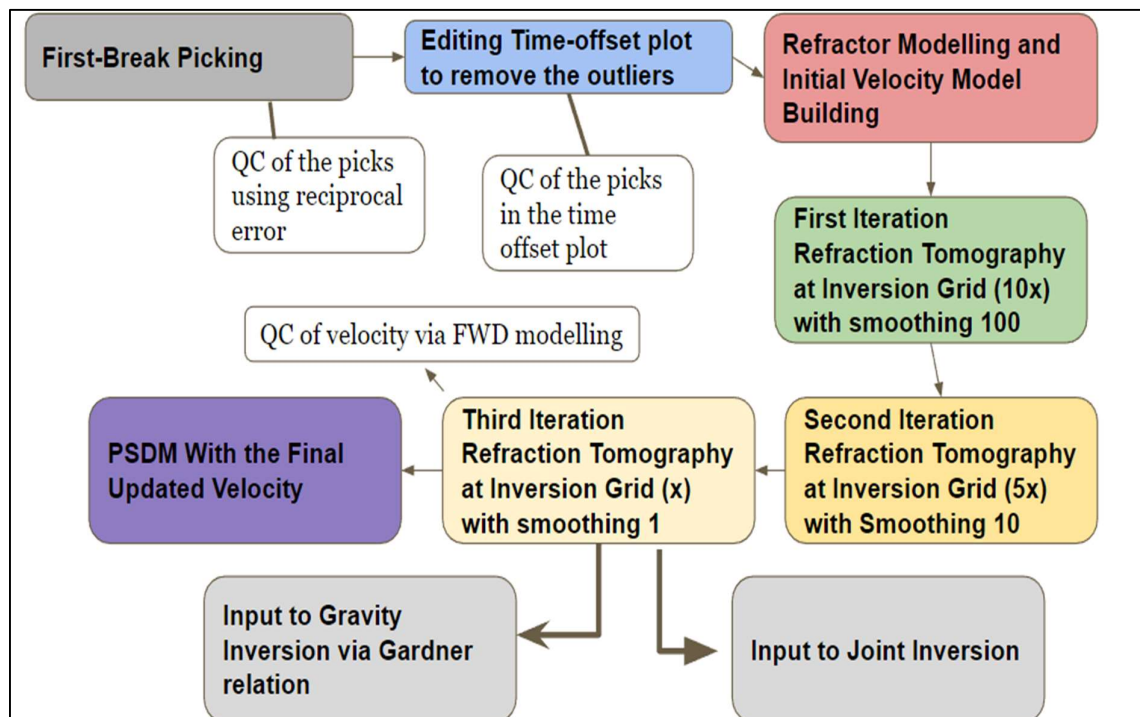
Fig. 1 Simplified flow diagram for joint inversion algorithm (*left*) and cooperative inversion (*right*) (Moorkamp et al, 2016b). The main difference between the two approaches is that for cooperative inversion one quantity that enters the coupling constraint (here seismic velocity, v) does not change throughout the inversion, while all quantities are adjusted withing the joint inversion.

Refraction Travel Time Tomography: A nonlinear refraction travel time tomography approach has

been used, based on the work of Jie Zhang and M.Tafi Toksoz (1998). The so-called *shortest path ray-tracing (SPR)* approach attempts to invert travel time curves, rather than travel times alone. So, SPR is the forward modelling approach used for tomography, and Tikhonov regularization has been used for non-linear inversion of the travel time data. Finally, the final solution is analysed using Monte Carlo methods of uncertainty estimation.

Seismic ray paths are obtained from travel time path, calculated through a grid network that represents the subsurface. The grids are connected via nodes. SPR Method can be achieved in **3 distinct steps** -

- Noting the time at nodes when an expanding wave front reaches there from the primary or secondary source.
- Finding the minimum travel time point along the wave front and taking this point as a secondary source.
- Expanding the wave front from this minimum time point.

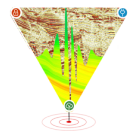


Workflow for Refraction Tomography

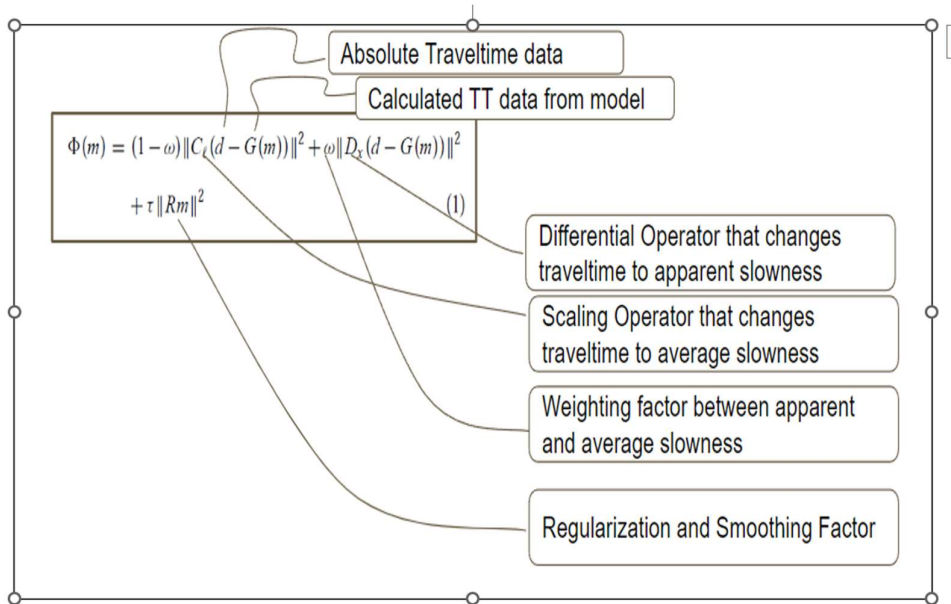
These three steps are repeated until the whole model is traced. SPR usually tends to produce a zigzag pattern in the homogenous or smooth velocity zones. The Sources of error in the SPR approach stem from space and angle discretization and these are independent of each other. The angle difference can be minimized by eliminating the difference between angles via optimization.

To invert the travel time and travel time curves, we solve a **nonlinear inverse problem**, starting from the initial model. The **travel times and ray paths** are updated iteratively without assuming any interfaces or velocity functionals. At the core, instead of inverting the absolute travel times, two different derived slowness (reciprocal of velocity) are inverted.

- **Average Slowness** (Travel time divided by ray lengths)
- **Apparent Slowness** (Travel time derivative w.r.t distance)

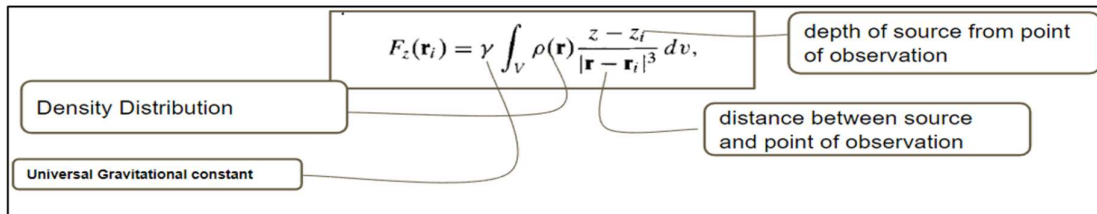


$$\begin{aligned} \Phi(m) &= (1 - \omega) \|C_t(d - G(m))\|^2 + \omega \|D_s(d - G(m))\|^2 \\ &\quad + \tau \|Rm\|^2 \quad (1) \\ &= (1 - \omega) \|\bar{d} - \bar{G}(m)\|^2 + \omega \|\bar{d} - \bar{G}(m)\|^2 \\ &\quad + \tau \|Rm\|^2 \quad (2) \\ &= (1 - \omega)S_1 + \omega S_2 + \tau S_3, \quad (3) \end{aligned}$$



Potential Inversion Gravity:

Based on the work of *Yaoguo Li and D. Oldenburg (1998)*, the 3D Gravity data can be inverted to obtain a physically possible and plausible density model volume. The Inversion Scheme includes a Forward Modelling Scheme and a comprehensive objective function, that is needed to be minimized to obtain a trustworthy result. For obtaining synthetic data for a given survey setup, the vertical component of the gravity field at any observation point “ \mathbf{r} ” can be calculated using the following integral equation



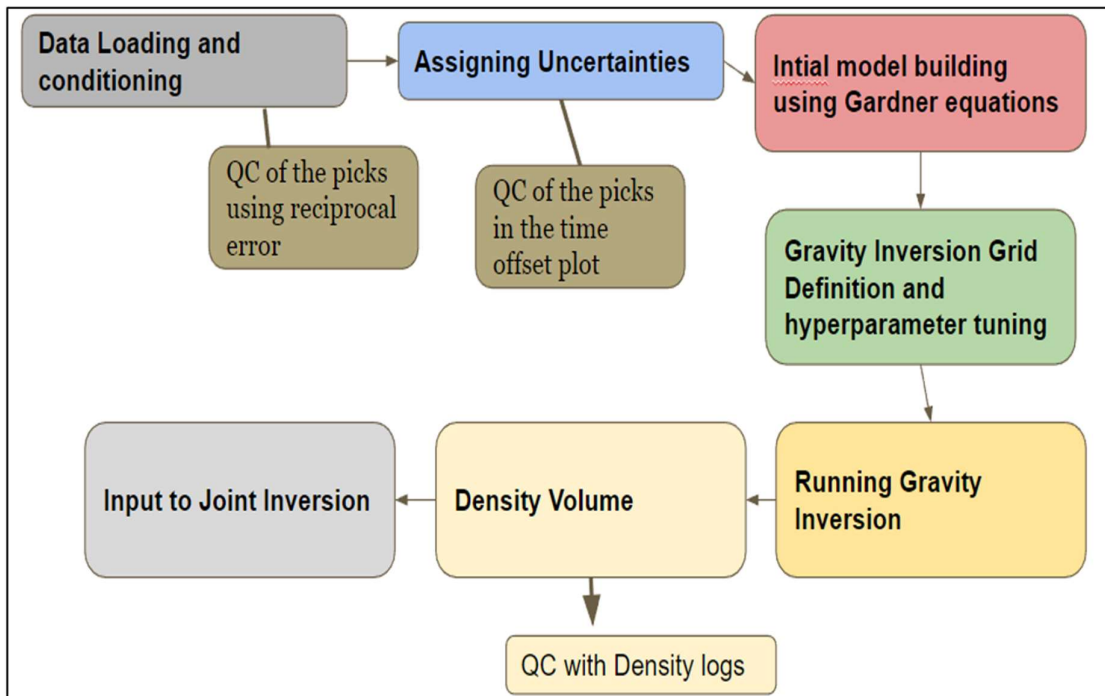
The objective function for Gravity Inversion is:

$$\phi(\mathbf{m}) = \phi_d(\mathbf{m}) + \beta \phi_m(\mathbf{m})$$

Where the data misfit is:

$$\phi_d(\mathbf{m}) = \|\mathbf{W}_d[\mathbf{F}(\mathbf{m}) - \mathbf{d}]\|^2$$

The ϕ_{small} is the smallness term. It defines how the model can vary from the reference model (priors) and ϕ_{smooth} defines how the gradient or Laplacian of the model varies compared to that of the reference model. 'β' here defines the relative contribution of data misfit and model regularization. It is a hyperparameter.



Workflow for Gravity Inversion

Joint Inversion of Gravity and Magnetic Data:

From the Works of Constable et. al. (1987), Oldenburg (1990), and Menke (2012), the general expression for an objective function for Joint Inversion is:

$$\phi_{JOINT} = \phi_d(m) + \beta\phi_m(m) + \lambda\phi_{COUPLING}$$

Φ_{JOINT} is the joint objective function, Φ_d is the data misfit, Φ_m model regularization, and $\Phi_{coupling}$ couples two different geophysical datasets. An additional **coupling term** is added to the objective function presented previously. **Via the Coupling term**, two different geophysical datasets are related to each other. Coupling is achieved by several strategies.

Joint inversion of gravity and magnetic data has been obtained using the following steps for an area in Cambay Basin using Magnum & Podium software.

1. Data pre-processing
2. Data Alignment
3. Forward modelling/Mesh generation
4. Joint Inversion Algorithm
5. Regularization

6. Optimization Algorithm
7. Model update & stopping criterion
8. Model validation & visualization

The coupling strategy used in our case are:

1. Correlation Coupling
2. Cross-correlation coupling

The result of the individual inversion (gravity & magnetic) and their joint inversion is given below.

Fig 1. Shows the Bouguer anomaly map along with the topography map of the area, which was prepared from the filed data

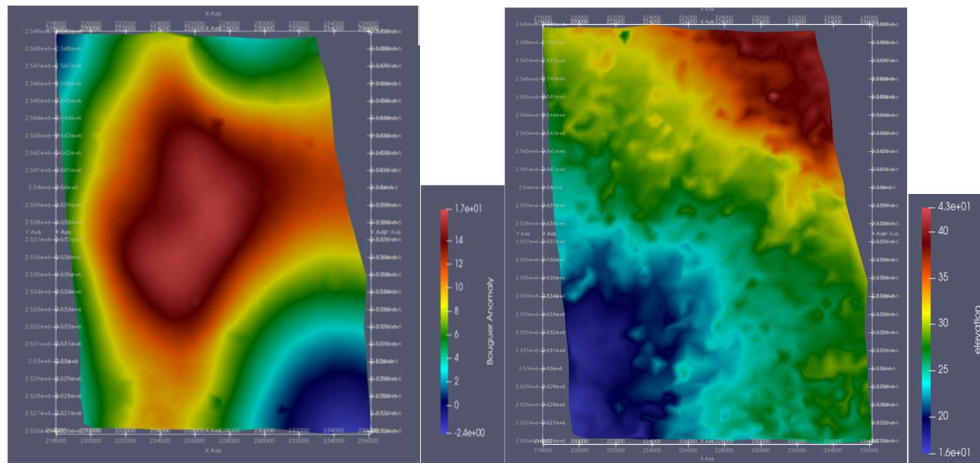


Fig1. Bouguer Anomaly map (left) and topography map (right) of the area.

The topography is Delaunay triangulated and the subsurface is tetrahedralized using “*Tetgen*” software which divides the subsurface into unstructured mesh of different dimension based on the location with respect to the target area. The initial model parameter, density in our case is assigned by the software for each cell along with the upper and lower bounds for the model parameter. Here, we have used local optimization for inversion in each case. The result of gravity inversion along with the field data is given below in Fig.2.

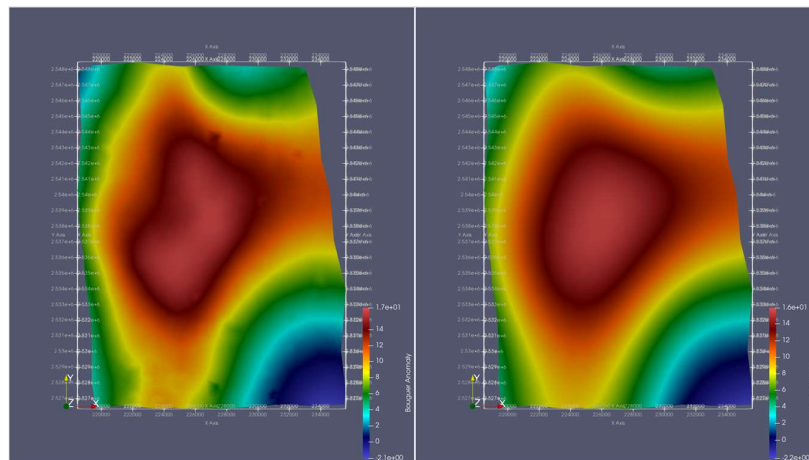


Fig2. Bouguer Anomaly map before (left) and after individual inversion (right).

In a similar way, the magnetic data was inverted independently which will be discussed later. The only additional parameter besides objective function and data misfit is the coupling strategy for joint inversion. Again, we have used local optimization to minimise the objective function. In our case, we have taken correlation, cross-correlation and fuzzy c means (FCM) coupling for carrying out the joint inversion. The result for the same is shown in Fig.3.

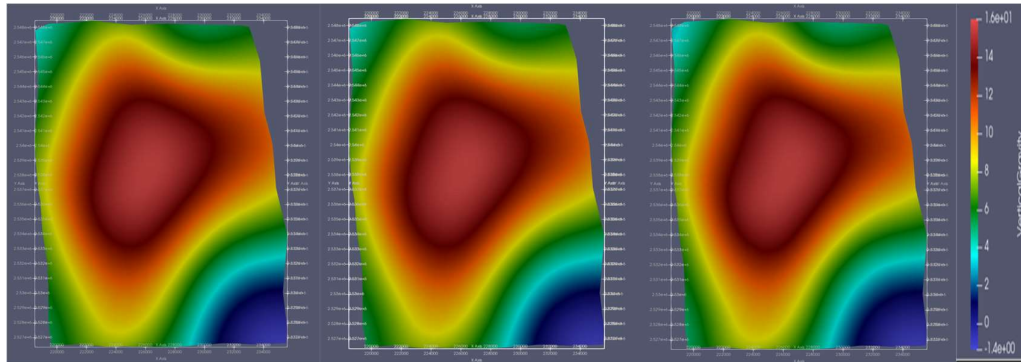


Fig3. Bouguer Anomaly map after joint inversion, the coupling parameter used correlation (left), cross-correlation (middle) and fuzzy c means (right).

Although, the result from the three-coupling strategy looks similar, however the use of FCM brings the inverted data closer to observed data. The density model obtained after joint inversion using FCM coupling is given below in Fig. 4. The model shows subsurface density variation up to 6 km.

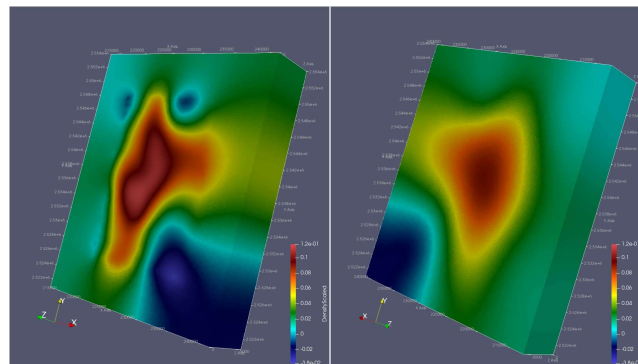


Fig4. 3D Density model; front view (left) and bottom view (right) after joint inversion using FCM coupling.

The magnetic anomaly for the same area has been analysed and in the similar way, unstructured mesh is used in forward modelling to obtain inversion result more closer to geology. The magnetic anomaly from the field data and topography map of the area is shown in Fig.5.

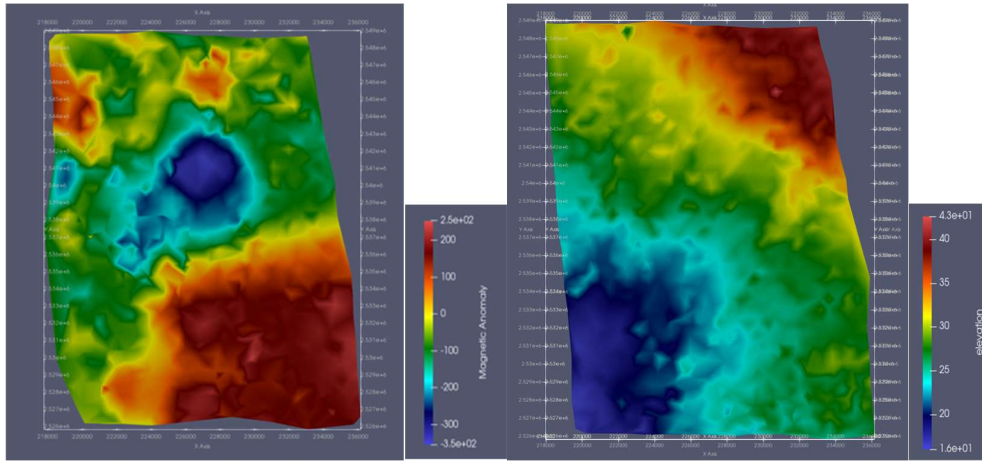


Fig5. Magnetic Anomaly map (left) and topography map (right).

Using local optimization again, we have performed magnetic inversion providing initial model values and its upper and lower bounds. The magnetic anomaly map after individual inversion looks quite similar to the one obtained directly from the magnetic field data, except its smoothness.

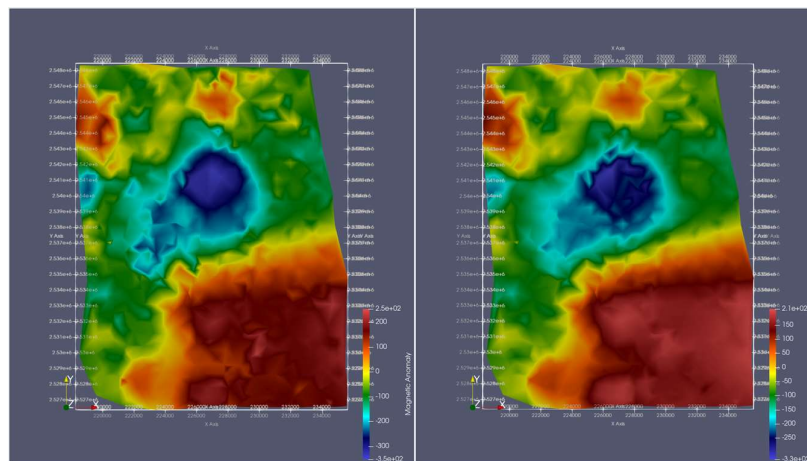


Fig6. Magnetic Anomaly map; before inversion (left) and after individual inversion (right).

After individual inversion, the joint inversion is performed with gravity data. The jointly inverted result for gravity has already been discussed mentioning the respective coupling parameter. Likewise, the result for magnetic inversion using correlation, cross-correlation and FCM coupling is shown below in fig. 7.

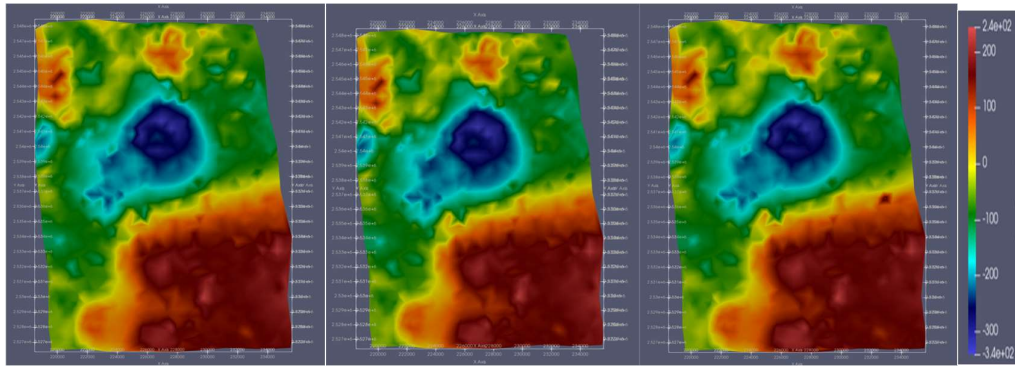


Fig.7 Magnetic Anomaly map after joint inversion; coupling parameter used correlation (left), cross-correlation (middle) and FCM (right).

Here, also the result from the three-coupling strategy looks similar, however the use of cross-coupling brings the inverted data closer to observed data. The susceptibility model obtained after joint inversion using cross-correlation coupling is given below in Fig.8. The model shows subsurface susceptibility variation up to 6 km.

The strategy adopted by Magnum & Podium for joint inversion was meant firstly to avoid the potential convergence problems and secondly to automatically adjust two tradeoff parameters, so that both datasets are fit to their desired level throughout the process. We can clearly see that the model obtained using the three different types of coupling produced very similar results, which increases the confidence level of the final model. These coupling measures make different assumption regarding the relationship between the physical properties. It may please be noted that we will use this joint inversion result with the seismic data for another joint inversion, as using three different data sets for making joint inversion is very complicated.

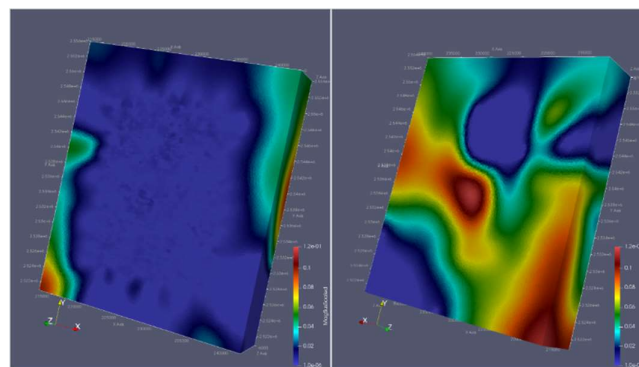


Fig.8 3D Susceptibility model, front view (left) and bottom view (right) after joint inversion using cross correlation coupling.

The Joint Inversion of Gravity and Seismic Data

In this case study, we had the two potential field data, namely gravity and magnetic data along with the seismic data to be inverted simultaneously. However due to computational and other limitations involving many parameters to be changed, only two datasets could be used for simultaneous Joint Inversion on larger scale. So, it was decided to first invert gravity and magnetic data jointly, thereafter, the final model the gravity which was obtained after SJI of gravity and magnetic was used with seismic data for their SJI. The reason for choosing gravity with seismic was for the fact that, seismic velocity is better related with the density. The availability of density data from several wells in the area was of great help in arriving at most accurate relationship between density and seismic velocity using gardener

relation. This methodology was adopted for the Joint Inversion of gravity, magnetic and seismic data from the Fold and Thrust Belt (FTB) area of North Eastern Part of the India using Geotomo & Paradigm software. Here, the three Coupling strategies used for our work are –

1. Cross-gradient (Structural Coupling)
2. Gardner Equation (Petrophysical Coupling)
3. Positivity Bound (Logarithmic Barrier)

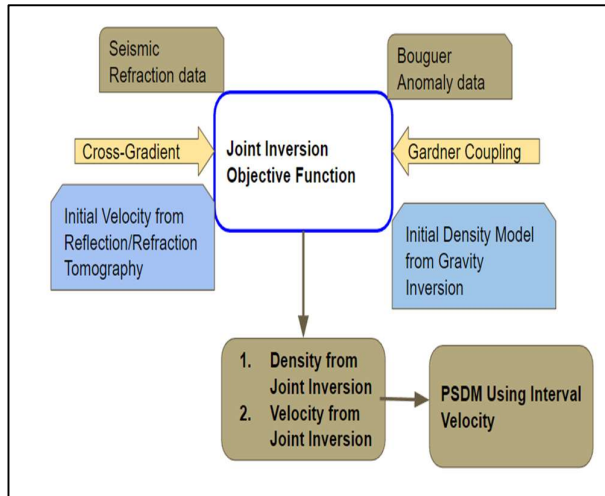


Fig. 9. Workflow for SJI of seismic and gravity

The schematic diagram showing the methodology for carrying out the joint inversion of seismic and gravity data is shown along side in fig. 9.

The first break travel time for all the good shots were picked and the near surface model for thickness and the velocity distribution were derived using the geotomo software. An example of the picked time is shown in the fig.10. The first break-time was inverted using the same software. This produced the synthetic first arrival times for all the shots. The comparison of the observed first break time and the synthetic first break time obtained after inversion is shown in the

fig.11. The close and focused alignment of the synthetic first break time obtained from the final model after inversion indicates the satisfactory working of the seismic inversion.

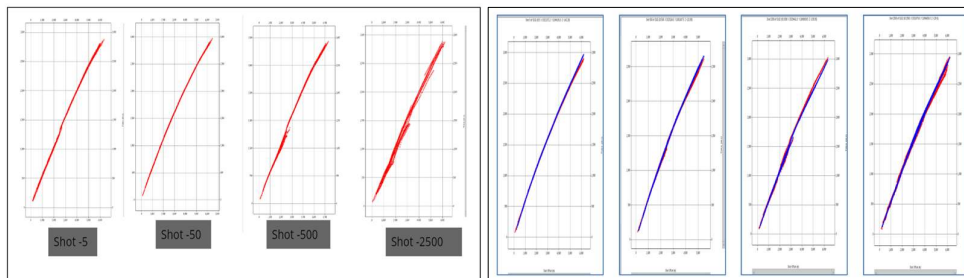


Fig.10. The picked First Break Travel time plot for different shot ID

Fig.11 Comparing synthetic FB picks generated from the Final model with true pick

The initial near surface refractor velocity model which was obtained from the first break solution is shown in the fig. 12. This model itself shows a heavy approximation of the velocity distribution. After final iteration of the first arrival travel time inversion, the near-surface velocity model got refined to the true geological model and is shown in the fig.13. The final isotropic velocity model during the depth imaging is shown fig. 14. Even after this final iteration of the isotropic depth imaging, the near surface velocity model had the scope of improvement, for this reason, the near surface interval velocity model from the final iteration of depth imaging was replaced with the one derived from the first break inversion. Few more iteration of the depth imaging was done with this new velocity model. The final interval velocity obtained using the first break inversion and depth imaging solution is shown in fig.15.

This model was used to migrate the data. The focusing of energy specially in the shallow part is quite improved with interval velocity model after SJI. The comparison of the depth migrated stack with conventional ISO velocity model and ISO interval velocity model after SJI is shown in fig. 16.

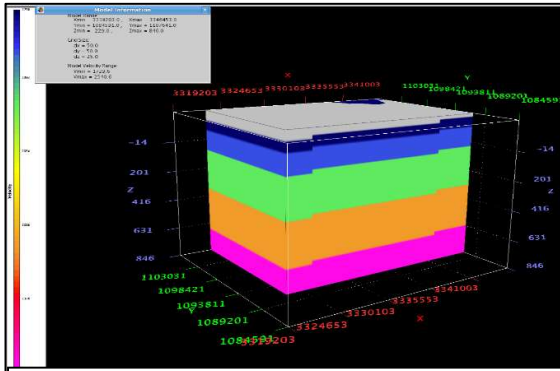


Fig.12 Initial Refractor Velocity Model

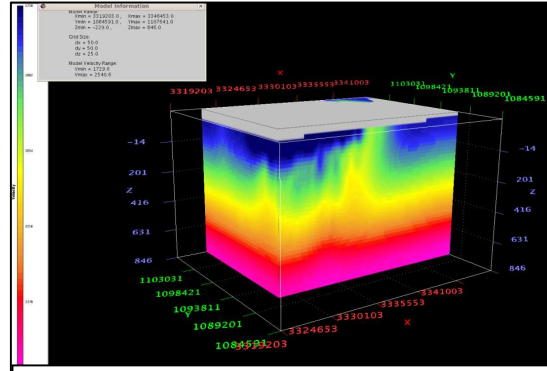


Fig. 13 Final Near Surface Model with grid size 50m x 50m x 25m

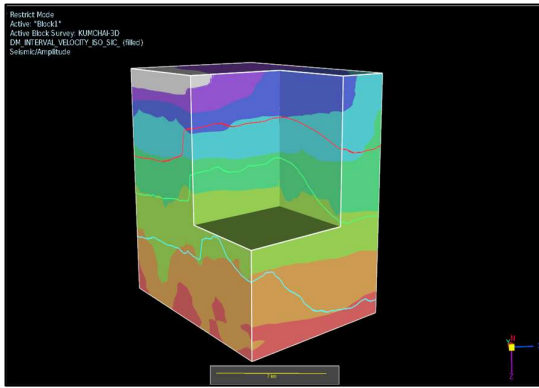


Fig.14 Isotropic Interval Velocity

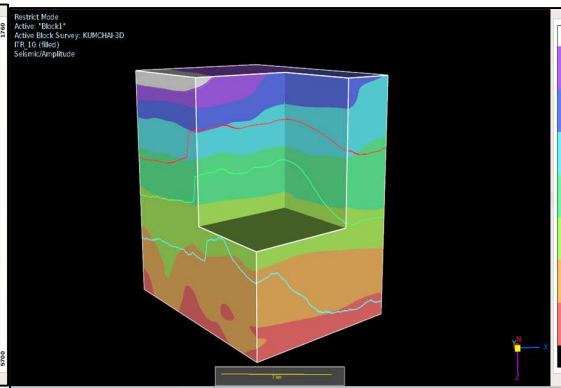


Fig.15 Joint inversion interval velocity.

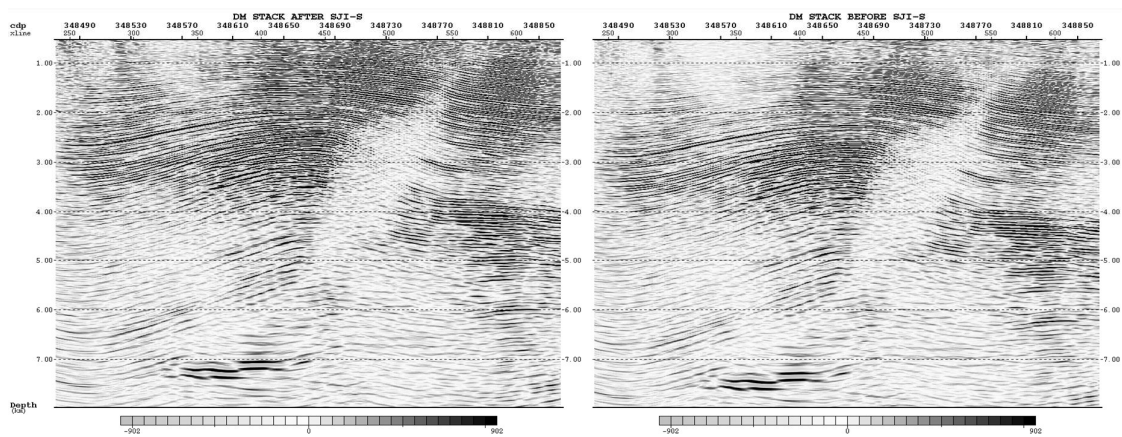
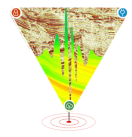


Fig.16 Migrated Stack with Isotropic Interval Velocity (left) and joint interval velocity (right).



Conclusion

The final gravity model, derived after the joint inversion of the potential field data (gravity and magnetic), were used to invert the first arrival time using SJI to get the final velocity model of the near surface. This final velocity model, were combined with the final velocity model derived from the depth imaging process. This new velocity model gave a superior subsurface image compared to the conventional result. This shows the significance of using the joint inversion wherever possible, especially in complex geological settings.

The undertaken study concluded with the joint inversion of the seismic data with the potential field data to arrive at better and more reliable result.

A comparison of the individual and joint inversion of the gravity and magnetic data also shows remarkable agreement in the result. This is the 1st time that we have successfully done this inversion on a larger area.

There is a greater scope of improvement in the result with increasing computational power and better algorithm which can utilize more constraint in arriving at final result.

Acknowledgement

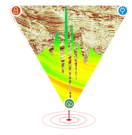
Authors express their sincere gratitude to ONGCL and Oil India Limited for providing all the support for carrying out the collaborative study on the Joint Inversion. Authors also express their gratitude to Dr. Peter G. Lelievre, Mount Allison University, Canada for continuous support at every step of this inversion with Magnum & Podium software.

Authors express their sincere gratitude to Department of Geophysics Banaras Hindu University for their best effort in making this industry-academia collaborative study, a reality.

Authors express their heartfelt thanks to Shivangi Srivastava, Research Assistant, Department of Geophysics, Banaras Hindu University for her unmatched effort to dive deep in MAGNUM and PODIUM that resulted to the best possible results in joint inversion.

References

1. Constable, S.C., Parker, R.L. and Constable, C.G., 1987. Occam's inversion: A practical algorithm for generating smooth models from electromagnetic sounding data. *Geophysics*, 52(3), pp.289-300.
2. Gallardo, L.A., Meju, M.A., 2003, Characterization of heterogeneous near-surface materials by joint 2D inversion of DC resistivity and seismic data. *Geophysics Res Lett* 30(13):1658. DOI:10.1029/2003GL017370.
3. Gallardo, L.A., Perez-Flores, M.A., Gomez-Trevino, E., 2003, A versatile algorithm for joint 3-D inversion of gravity and magnetic data. *Geophysics* 68:949–959.
4. Zhang, J., ten Brink, U.S. and Toksöz, M.N., 1998. Nonlinear refraction and reflection travel time tomography. *Journal of Geophysical Research: Solid Earth*, 103(B12), pp.29743-29757.
5. Kozlovskaya, E., 2001, Theory, and application of joint interpretation of multimethod geophysical data. Ph.D. dissertation, University of Oulu, Oulu, Finland.
6. Lines, L.R., Schultz, A.K., Treitel, S., 1988, Cooperative inversion of geophysical data. *Geophysics* 53:8–20.



7. Lelièvre, P.G., Farquharson, C.G. and Hurich, C.A., 2011. Computing first-arrival seismic traveltimes on unstructured 3-D tetrahedral grids using the fast marching method. *Geophysical Journal International*, 184(2), pp.885-896.
8. Li, Y. and Oldenburg, D.W., 1998. 3-D inversion of gravity data. *Geophysics*, 63(1), pp.109-119.
9. Manglik, A., Verma, S.K., Singh, K.H., 2009, Detection of sub-basaltic sediments by a multiparametric joint inversion approach. *J Earth Syst Sci* 118:551–562.
10. Max Moorkamp, Bjorn Heincke, Marion Jegen, Alan W. Roberts and Richard W. Hobbs (2010) A framework for 3-D joint inversion of MT, gravity, and seismic refraction data. *Geophysical J. Int.* (2011) **184**, 477–493
11. Max Moorkamp (2017). Integrating Electromagnetic Data with Other Geophysical Observations for Enhanced Imaging of the Earth: A Tutorial and Review. *Surv Geophysics* (2017) 38:935-962
12. Oldenberg, H. and Pischel, R., 1990. Thera-and Therī-Gāthā, with appendices by KR Norman and L. Alsdorf.
13. Vozoff, K., Jupp, D.L.B., 1975, Joint inversion of geophysical data. *Geophysics J R Astr Soc* 42:977–991.